HHS Public Access

Author manuscript

Hum Brain Mapp. Author manuscript; available in PMC 2018 February 01.

Published in final edited form as:

Hum Brain Mapp. 2017 February ; 38(2): 1009–1024. doi:10.1002/hbm.23435.

Twin–Singleton Developmental Study of Brain White Matter Anatomy

Neda Sadeghi[1,*], **John H. Gilmore**[2], and **Guido Gerig**[3]

[1]Section on Quantitative Imaging and Tissue Sciences, Eunice Kennedy Shriver National Institute of Child Health and Human Development, National Institutes of Health, Bethesda, MD, USA

[2]Department of Psychiatry, University of North Carolina, Chapel Hill, NC, USA

[3]Tandon School of Engineering, Department of Computer Science and Engineering, NYU, Brooklyn, USA

Abstract

Twin studies provide valuable insights into the analysis of genetic and environmental factors influencing human brain development. However, these findings may not generalize to singletons due to differences in pre- and postnatal environments. One would expect the effect of these differences to be greater during the early years of life. To address this concern, we compare longitudinal diffusion data of white matter regions for 26 singletons and 76 twins (monozygotic and dizygotic) from birth to 2 years of age. We use nonlinear mixed effect modeling where the temporal changes in the diffusion parameters are described by the Gompertz function. The Gompertz function describes growth trajectory in terms of intuitive parameters: asymptote, delay, and speed. We analyzed fractional anisotropy (FA), axial diffusivity (AD), and radial diffusivity (RD) for 21 regions of interest (ROIs). These ROIs included areas in the association, projection, and commissural fiber tracts. We did not find any differences in the diffusion parameters between monozygotic and dizygotic twins. In addition, FA and RD showed no developmental differences between singletons and twins for the regions analyzed. However, the delay parameter of the Gompertz function of AD for the anterior limb of the internal capsule and anterior corona radiata was significantly different between singletons and twins. Further analysis indicated that the differences are small, and twins “catch up” by the first few months of life. These results suggest that the effects of differences of pre- and postnatal environments between twins and singletons are minimal on white matter development and disappear early in life.

Keywords

twins; longitudinal brain imaging; early brain development; DTI; nonlinear mixed effects modeling; diffusion; white matter; Gompertz function

[*]Correspondence to: Neda Sadeghi. neda.sadeghi@nih.gov.

INTRODUCTION

Twin studies have contributed substantially to our understanding of the heritability of many neuropsychiatric and neurodevelopmental disorders [Kendler, 2001]. Comparing identical (monozygotic twins, MZ) and fraternal (dizygotic, DZ) twins allows researchers to estimate contributions of heritability and environment to individual differences [Chiang et al., 2011; Gilmore et al., 2010; Jahanshad et al., 2013; Lee et al., 2015; Peper et al., 2007]. However, it might be difficult to generalize these findings to the singletons population, as twins face additional challenges during early development. The intrauterine environment of twins might be considered suboptimal as twins share the womb and compete for nutritional resources [Hulshoff Pol et al., 2002; Knickmeyer et al., 2011]. Postnatal environment might also be suboptimal as twins share family resources and compete for attention [Hay and O'Brien, 1983].

Some studies have suggested the nongeneralizability of twin studies to singletons as they have found differences in cognitive measures [Hay and O'Brien, 1983; Nathan and Guttman, 1984]. However, more recent studies have found no differences in IQ between twins and the singleton population, suggesting that findings in twin studies can be generalized to the singleton population [Posthuma et al., 2000]. Other studies have looked at differences between brains structure/size of twins and singletons. Hulshoff Pol et al. (2002) compared brain anatomy of twins and singletons in the adult population (mean age = 30.7, sd = 9.6 years) and found no differences in white matter volume after correcting for intracranial volume. Ordaz et al. studied the brain morphometry between twins and singletons in children and adolescents (mean age = 11, sd = 3.6) and found no significant differences between the two groups in ventricular, white and gray matter lobar volumes. However, it is possible that the adverse effect of pre- or perinatal period gradually diminishes. Knickmeyer et al. (2011) studied a younger cohort; subjects were at the first month of life where the effects of suboptimal in utero environment might be more pronounced. They found increased frontal white matter volumes in twins compared to singletons, but no differences were observed in intracranial volume, total white matter, and ventricle volumes between twins and singletons. In the same study, significant differences in gray matter development in MZ twins compared to DZ twins and singletons were observed, suggesting gray matter development is delayed in MZ twins in utero, and they experience "catch up" in the first month of life [Knickmeyer et al., 2011].

In addition to morphometric studies, developmental studies have utilized diffusion tensor imaging (DTI) to gain a better understanding of white matter development [Basser et al., 1994, Pierpaoli et al. 1996]. DTI-derived metrics have been shown to correlate with maturation of underlying tissue. Most of the early brain development studies have been based on cross-sectional data [Dubois et al., 2008; Gao et al., 2009; Hermoye et al., 2006; Huppi et al., 1998; Mukherjee et al., 2002]. However, more recently, there have been studies based on longitudinal DTI data [Geng et al., 2012; Sadeghi et al., 2013]. Longitudinal studies can better characterize development, have more power in detecting differences, and are better suited to answer questions related to development. We were not able to find any other DTI studies of early brain development that compare development of singletons and twins. We were able to find one twin DTI study [Chen et al., 2009] that compared growth

patterns of monozygotic and dizygotic twins in a very limited number of ROIs (posterior limb of the internal capsule, external capsule, and the centers of genu and splenium in an axial slice), and found no effect of zygosity.

As part of our brain development imaging studies, we have acquired a dataset with a total of 238 MRI scans of longitudinal imaging data of twins and singletons ranging from few weeks to 2 years of age. Given the challenges of multimodal MR imaging of infants at this early age, including dual contrast anatomical MRI and DTI, this represents a unique dataset covering the critical period of rapid development and growth. In the study reported here, we focus on the presentation of longitudinal models of brain white matter diffusivity to assess eventual differences on trajectories of early brain development between twins and singletons. We hypothesize that the effect of prenatal environment, if any, would be more noticeable at the early age as was shown previously by [Knickmeyer et al. (2011)]. It is important to find out whether developmental trajectories as represented by DTI in twins are similar to those in singletons. For example, can we include twin subjects in singletons studies? Can we generalize twin study findings to singletons? To answer these questions, we study the developmental trajectory of subjects as represented by DTI in a cohort of twins and singletons aged 2 weeks to 2 years.

MATERIALS AND METHODS

Subjects

Mothers were recruited during their second trimester of pregnancy from clinics at the University of North Carolina for a longitudinal twin study. In total, 26 singletons and 76 twins who had DTI scans were used for this study. There are 28 twin pairs (DZ = 14, MZ = 14) and 20 “single” twins (DZ = 12, MZ = 8). “Single” twins are twins for whom usable scans from the other twin pair were not obtained. Demographic data are provided in Table I. Infants were scanned at about 3 weeks, 1 year, and 2 years without sedation during natural sleep. Not all subjects had all three scans available. The distribution of scans is shown in Figure 1. This study was approved by the Institutional Review Board of the University of North Carolina School of Medicine.

Image Acquisition

All images were acquired using a 3T Allegra head-only MR system using a single shot echo-planar spin echo diffusion tensor imaging sequence with the following parameters: TR = 5200 ms, TE = 73 ms, a slice thickness of 2 mm, and in-plane resolution of 2×2 mm^2. One image without diffusion gradients ($b = 0$) along with six gradient directions with a b-value of 1000 mm^2/s were acquired. The sequence was repeated five times for an improved signal-to-noise ratio. All DWIs were checked and corrected for motion artifacts using the DTIChecker tool.[1] Tensor maps were calculated for each DTI scan using a weighted least squares tensor estimation on the images that have been averaged over sequence repeats [Salvador et al., 2005]. T2-weighted structural images were obtained using a turbo spin echo sequence with TR = 7 s, TE = 15 and 90 ms, a slice thickness of 1.95 mm, and in-plane resolution of 1.25 ×

[1] http://www.ia.unc.edu/dev/download/dtichecker

1.25 mm^2. T2W and baseline DWI of all the subjects' scans were skull stripped using the Brain Extraction Tool (BET) [Smith, 2002].

Image Processing

Image registration and processing were done in a similar fashion as described by Sadeghi et al. [2013]. Due to significant contrast changes in early brain development, we utilized two registration frameworks: a method by Joshi et al. [2004] to build an unbiased atlas and IRTK soft-ware[2] for intrasubject registration. Unbiased atlas building was used to provide a mapping between individuals to the template atlas [Joshi et al., 2004]. The atlas was built from the population of data in the study as the average template. All individuals' scans were first mapped to their year 1 T2W scan via the linear and nonlinear registration method of Rueckert et al. [1999] and subsequently to the atlas via deformation maps obtained during the atlas building procedure. The tensors were registered to the atlas using transformations obtained by registering the DTI baseline (B0) images to T2W images. For each subject, the transformations obtained during intrasubject registration were converted to displacement fields and combined with the displacement fields obtained during template creation, this combined displacement field was used to warp the diffusion tensor of each subject to the template with one interpolation ensuring minimal degradation of the quality of the tensor metrics. Tensor maps were calculated using the weighted least squares estimation method and transferred to the atlas using finite strain reorientation and Riemannian interpolation [Alexander et al., 2001; Fletcher and Joshi, 2007; Pennec et al., 2006]. In this study, we extracted the following diffusion measures from the tensor maps: axial diffusivity (AD = λ_1), radial diffusivity ($\mathrm{RD}=\frac{\lambda_2+\lambda_3}{2}$), and fractional anisotropy ($\mathrm{FA}=\sqrt{\frac{1}{2}}\frac{\sqrt{(\lambda_1-\lambda_2)^2+(\lambda_1-\lambda_3)^2+(\lambda_2-\lambda_3)^2}}{\sqrt{\lambda_1^2+\lambda_2^2+\lambda_3^2}}$), where λ_i are the eigenvalues of the tensor sorted from largest to smallest.

Regions of Interest

We used the white matter label map that is developed and disseminated by Mori et al. [2008] to define anatomical regions of interest (ROIs). This label map was mapped to the template atlas via linear followed by nonlinear b-spline registration [Rueckert et al., 1999]. We selected 21 anatomical regions in the atlas space as shown in Figure 2. The labeling of regions in the atlas space allowed automatic partitioning of each subject's scans into the different anatomical regions (Fig. 3). The white matter regions included regions in projection, association, and commissural fiber tracts. Regions in commissural tracts included body, genu, and splenium of corpus callosum. Regions in the projection fiber tracts were anterior and posterior limb of internal capsule, posterior thalamic radiation, and anterior, superior, and posterior corona radiata. Regions in association fiber tracts included external capsule and superior longitudinal fasciculus.

[2] http://www.doc.ic.ac.uk/dr/software

Statistical Analysis

We use nonlinear mixed effects (NLME) to estimate trajectories of development as shown in DTI within anatomical ROIs [Pinheiro, 1994]. White matter is known to mature more rapidly in the first year of life than in the second, with a continued maturation but at a much slower rate into adulthood [Dubois et al., 2008; Geng et al., 2012; Hermoye et al., 2006; Sadeghi et al., 2013]. This type of development favors functions that have asymptotic behavior such as exponential, logistic, or Gompertz. We have demonstrated [Sadeghi et al., 2013; Sadeghi, 2013] that the parametric Gompertz function is well suited for modeling early brain development, $y = f(\phi, t) = \phi_1 \exp\{-\phi_2\phi_3^t\}$. Moreover, the parameters of the Gompertz function also provide intuitive parameterization of growth: ϕ_1 denotes asymptote, ϕ_2 is the delay, and ϕ_3 is the exp (−speed). To accommodate the differences in gestational age between twins and singletons, we use gestational age as the predictor variable. The Gompertz function was calculated by fitting the diffusion parameters over the gestational age range available for all subjects, i.e., gestational age minus minimum gestational age over all subjects.

We model the longitudinal changes via a nonlinear mixed effects model rather than a nonlinear least square as a mixed effects model fits a group developmental trajectory while accounting for variability among individuals. Mixed effects models provide a powerful and flexible environment for analyzing longitudinal data by properly accounting for the intercorrelation among observations on each subject [Diggle et al., 2002]. In the mixed effects model, the observed data are assumed to be a combination of fixed effects, parameters associated with the entire population (or subpopulation), and random effects that are specific to an individual drawn at random from the population. Correlation among repeated scans of an individual is accounted for by incorporating random effects in the model. For twins, we model a twin pair as a random effect to capture correlation between subjects within twin pairs. This allows both twins to be included in the analysis without violating the independence assumption. We also take advantage of data of “single” twins in our study as the main objective of our study is to compare twins to singletons, which does not require both twins to be present in the study.

Mixed effects model also results in a group trend (fixed effects) that better reflects individual progress on average compared to a least square fit. We model asymptote, delay, and speed of the Gompertz function as fixed effects. Additionally, asymptote and delay are modeled as random effects. We set one of the random effects to zero to reduce the number of random effects in the model. As we have a maximum of only three time points per subject, including an additional random effect may create problems in the estimation of the parameters. We previously showed that a model with asymptote and delay as random effects showed the lowest Akaike Information Criterion (AIC), where the lowest AIC indicates a better model fit [Akaike, 1974; Sadeghi, 2013].

Separate NLME models were fit for FA, AD, and RD of each ROI for each group (MZ, DZ, and singletons). The hypothesis of wether developmental trajectories between twins and singletons are the same was evaluated by performing a *t*-test on the fixed parameters of the Gompertz function [Lindstrom and Bates, 1990; Sadeghi et al., 2013]. A false discovery rate

procedure was used to control for type 1 error at the level of $q < 0.05$ [Benjamini and Hochberg, 1995].

Among the 102 subjects included in the analysis, 92 had scans at neonatal age, 97 scans at 1 year, and 49 scans at 2 years. The mixed effects framework accommodates missing time points and unbalanced data. Using the nonlinear mixed effects model and Gompertz function allows us to incorporate the variable age that is present in our cohort and to model nonlinear changes in diffusion metrics that are present at this early age. The main advantage of this approach is that subjects do not need to have observations at exactly the same time points (hence the data can be unbalanced). Additionally, we have included data with single time points in our study as is was previously shown that including such additional data points significantly improves the accuracy of a model fit in a mixed effects approach [Bernal-Rusiel et al., 2013].

RESULTS

A comparison of mean trajectories between monozygotic and dizygotic twins indicated very similar trajectories. No significant differences were found between the growth curves of MZ and DZ in terms of Gompertz parameters of asymptote, delay, and speed for any of the diffusion measurements. For example, Figure 4 shows the FA, AD, and RD of the right external capsule for monozygotic and dizygotic twins, where there is no difference between the two groups. To further investigate whether twins and singletons show any developmental differences, DZ and MZ individuals were combined as there were no differences in their growth trajectories.

Gestational age was controlled for in the analysis as twin subjects are generally born earlier than singletons. In this study, twins were born about 30 days earlier than singletons on average. To ensure that the observed differences between twins and singletons are not due to gestation age differences, gestation age at the time of the MRI scan was taken into account rather than age. Table I shows the gestational age at birth and at the time of the first MRI scan for twins and singletons.

When comparing the combined twin group to singletons, FA and RD of all the regions showed similar trajectories. The estimates of Gompertz parameters of FA and RD for twins and singletons are shown in Tables II and III, where no significant differences were found between average trajectories. AD of all the regions also showed similar trajectories between twins and singletons, with a few exceptions. The following regions showed significant differences in the delay parameter of the AD: the right and left anterior limb of the internal capsule and the right and left anterior corona radiate (Figure 5). There were no significant differences in asymptote and speed parameters of AD between these two groups for any of the regions analyzed. Table IV shows the estimated Gompertz parameters of AD for twins and singletons. In the regions in which the delay parameter was significant, AD reached the same level as singletons by the first 3 months, as though twin subjects “catch up” to singletons shortly after birth.

The changes from birth to 2 years in AD for the anterior limb of the internal capsule (ALIC) and the anterior corona radiata (ACR) are shown in Figure 5 the changes in the delay parameter were significantly different in the two groups. The delay parameter for the right and left ALIC is −0.19 (95% confidence interval (CI): −0.21 to −0.17) and −0.22 (95% CI: −0.24 to −0.20) in singletons vs. −0.24 (95% CI: −0.29 to −0.20) and −0.27 (95% CI: −0.31 to −0.22) in twins (Table IV). The delay parameter relates the initial values of a diffusion metric to its final value (i.e., estimated values for the asymptote compared to estimated diffusion values at birth). For diffusion values that follow a decreasing pattern during the development such as AD and RD and have similar asymptotic values for both singletons and twins, smaller delay values indicate higher AD and RD at earlier gestational age as shown in Figure 5. The majority of the regions for AD showed a similar trend where the delay parameter was smaller for twins compared to singletons. However, after multiple comparisons correction, most of the regions did not show any significant difference between the two groups. The summary of *P*-values for all the regions and all diffusion metrics are shown in Appendix A. Some of the regions showed very similar trajectories between twins and singletons. For example, Figure 6 shows the trajectories for FA, RD, and AD of the posterior limb of the internal capsule where the trajectories are remarkably similar.

Figure 7 shows the relative difference of AD between twins and singletons computed at 39 and 43 weeks of gestation. At 39 weeks of gestation, all the regions show higher AD for twins compared to singletons. To assess whether this is a global effect, we performed the same analysis (comparison of twins and singletons) on the combined ROIs. There was a significant difference of the delay parameter of AD between singletons and twins, whereas we did not find any significant difference between FA and RD (Table V). It seems that the delay in the AD parameter for twins is a global phenomenon of the set of interior white matter ROIs but shows its strongest effect in the anterior regions of this set such as the anterior limb of the internal capsule and the anterior corona radiata.

Since there seem to be differences around the time after birth that disappear quickly, we performed additional tests using only the first time point. Group differences were tested on the combined ROIs. Figure 8 shows the FA, AD, and RD of twins and singletons with respect to gestational age. There is no difference between twins and singletons considering gestational age as a covariate in the linear model for any of the diffusion metrics that we analzyed. However, by considering longitudinal data and modeling with the Gompertz function, we were able to detect differences between the two groups in the delay parameter of the Gompertz function for AD (Table V).

DISCUSSION

This study compared longitudinal development of white matter regions between MZ and DZ twins, as well as twins and singletons. We compared growth trajectories in regions of projection, association, and commissural fiber tracts. Regions in projection fibers included areas of the internal capsule and corona radiata. Other regions include superior longitudinal fasciculus and external capsule for association tracts, and genu, body, and splenium of corpus callosum for commissural tracts. Our findings suggest that there are no differences in DTI measurements between MZ and DZ twins. The average growth trajectories for MZ and

DZ are very similar, with some regions almost identical. We were able to find only one other DTI study that compared growth trajectories of MZ and DZ [Chen et al., 2009]. Our result is consistent with their findings [Chen et al., 2009] where they analyzed FA and MD of four small regions and found no differences based on the zygosity.

Subsequently, we combined MZ and DZ twins as there were no differences in their growth trajectories, and we compared twins to singletons. For the majority of the regions, the trajectories of singletons and twins are also very similar. FA and RD did not differ between twins and singletons in any of the regions that we analyzed after correction for multiple comparisons.

However, twins and singletons did exhibit differences in AD measures in the anterior limb of the internal capsule and the anterior region of the corona radiate (Table AI and Fig. 7). There were significant differences in the delay parameter of the Gompertz function for these regions (higher AD values at lower age for twins), indicating that twins were delayed compared to singletons. However, there were no significant differences in the asymptote parameter of the Gompertz function, suggesting that the twin–singleton differences observed early on in these regions disappear by early childhood. Figure 7 shows the relative difference of AD between twins and singletons computed at 39 and 43 weeks of gestation, which indicates that twins experience a period of “catch-up” growth. We chose 39 weeks as a reference as it is considered full-term pregnancy, and we compared it to our modeling at 43 weeks which is roughly a month after, to demonstrate how quickly twins will “catch-up.”

Even though we were not able to find DTI studies of early brain development between twins and singletons, we were able to find studies that have analyzed differences in brain morphology between these two groups. For example, in a study by Ordaz et al. [2010], they found no differences in gray and white matter lobar volumes, ventricular volume, and area of corpus callosum between twins ($n = 185$) and singletons ($n = 167$). Subjects’ age ranged from 4.6 to 19.5 years. Another study, by Hulshoff Pol et al. (2002) compared 112 twins and 34 of their healthy nontwin siblings (mean age of 30.7, sd = 9.6 years), the only significant difference was found in white matter volume; however, once intracranial volume was taken into account, the white matter volume was no longer significantly different between twins and singletons.

Knickmeyer et al. [2011] also found no differences in gray matter, white matter, and cerebrospinal fluid (CSF) volumes between twins ($n = 154$) and singletons ($n = 136$) during the first month after birth. However, when the twin groups were divided by zygosity, they found the slope of total gray matter volume to be steeper for MZ twins compared to DZ twins, as though they go through a period of “catch-up.”

Our results, similar to previous studies, show more similarities between twins and singletons than differences, and it seems if there are any differences, they resolve quickly in early childhood. These observations are similar to other measurements such as height and weight that have been shown to be different at birth between singletons and twins, but quickly diminish [Buckler and Green, 2004; Wilson, 1974]. Some of the differences are due to the shorter gestation of twins; however, once the gestational age is taken into account, some of

these differences disappear [Buckler and Green, 2004]. Additionally, recent studies of academic performance and IQ of adolescence and adults have shown no differences between twins and singletons [Christensen et al., 2006; Posthuma et al., 2000].

There are some limitations to our study. The number of gradient directions in this study was limited to six directions; however, each direction was repeated five times. Since the establishment of the protocol for this study, many have advocated use of more directions in favor of more repeats [Jones, 2004]. Per these recommendations, the images acquired during the second phase of this study are being acquired in 42 directions. Ni et al. [2006] did a comparison of diffusion-derived parameters of 50 healthy volunteers acquired in 1.5 T MRI with three protocols: (number of directions/number of repeats = 6/10, 21/3, 31/2). They did not find any significant differences in FA between these three protocols, however, they reported that 6-directions protocol yielded higher values for λ_1 and λ_2 and lower values for λ_3 compared to 21- and 31-directions but the effect size was small. As imaging modalities improve, diffusion metrics can be estimated with higher accuracy. However, as both twins and singletons were scanned with the same protocol, we do not expect any bias on the group comparison based on using only six gradient directions.

It is also worth noting that our analysis depends on accurate registration of scans across subjects and within a subject. In this study, we used ROI-based analysis as we expect it would be more robust compared to voxel-based analysis. Nonetheless, improved registration algorithm will potentially improve the accuracy of our models.

Substantially more scans were available at neonatal and year 1 ages compared to year 2. One of the advantages of utilizing mixed effects model is its ability to handle missing time points. Missing data can be categorized into three groups: missing completely at random (MCAR), missing at random (MAR), and not missing at random (NMAR). When missing data is MCAR or MAR, the estimated parameters will not be biased. In our case, we have more missing time points at year 2 compared to neonate and year 1. When missing data is not related to the value of diffusion parameter (i.e., FA, RD, and AD), it is MCAR or MAR and the fixed effect parameters will not be biased. In this study, we suspect subjects missed the scans at the later time points due to the loss of interest in the study or moving away. We also performed simulation studies that shows the missing time points have minimal effect on the estimates of fixed effect parameters (Appendix B).

In summary, nonlinear mixed effects modeling provides a powerful method to analyze longitudinal data where data can have missing time points and uneven spacing between observations. In addition, it makes use of single time points for improved estimation of intersubject variability. The use of the Gompertz function appropriately models the rapid nonlinear changes that we observe early in life. Using this approach enabled us to find small, but significant differences in the delay parameter of the Gompertz function for AD of a few white matter regions, while growth trajectories of FA and RD showed no differences. Significant differences were observed only in the AD in the anterior limb of the internal capsule and the anterior region of the corona radiata; however, these differences seem to disappear early in life. No effect of zygosity on growth trajectories was found. The findings suggest that twins can be included with singletons in DTI studies of early brain

development, but researchers should control for gestational age and be cautious when the gestation age is less than 43 weeks.

Acknowledgments

Contract grant sponsor: NIH; Contract grant number: R01 MH070890, R01 HD05300 and Conte Center MH064065; Contract grant sponsor: NIH; Contract grant number: NA-MIC U54 EB005149 and U01 NS082086

APPENDIX A

SUMMARY OF P-VALUES AND EFFECT SIZE OF SINGLETON–TWIN COMPARISON

Tables AI, AII, and AIII display the *p*- and *q*-values for singletons–twins comparison of FA, RD, and AD.

Tables AIV, AV, and AVI display the effect size for singletons-twins comparison of FA, RD, and AD. Effect size is calculated based on Cohen's *d* which is defined as $d=\frac{\overline{x}_1-\overline{x}_2}{s}$, $\bar{x}_1$ and $\bar{x}_2$ are the estimated population parameters (i.e., asymptote, delay, and speed) for singletons and twins, respectively. *s* is the pooled standard deviation, $s=\frac{\sqrt{(n_1-1)s_1^2+(n_2-1)s_2^2}}{n_1+n_2-2}$, and n_1 and n_2 are the number of subjects in each group.

TABLE AI

P-values for singleton–twin comparison of fractional anisotropy (FA)

	p-value			*q*-value		
Regions of interest	**Asymptote**	**Delay**	**exp(−Speed)**	**Asymptote**	**Delay**	**exp(−Speed)**
Genu of corpus callosum	0.46	0.75	0.29	0.64	0.94	0.54
Body of corpus callosum	0.56	0.68	0.91	0.64	0.94	0.98
Splenium of corpus callosum	0.64	0.43	0.99	0.64	0.75	0.98
Anterior limb of internal capsule R	0.05	0.07	0.26	0.58	0.39	0.54
Anterior limb of internal capsule L	0.23	0.94	0.54	0.64	0.94	0.78
Posterior limb of internal capsule R	0.52	0.25	0.90	0.64	0.54	0.98
Posterior limb of internal capsule L	0.30	0.28	0.98	0.64	0.54	0.98
Retrolenticular part of internal capsule R	0.33	0.84	0.76	0.64	0.94	0.96
Retrolenticular part of internal capsule L	0.64	0.59	0.78	0.64	0.89	0.96
Anterior corona radiata R	0.54	0.13	0.30	0.64	0.49	0.54
Anterior corona radiata L	0.62	0.07	0.23	0.64	0.39	0.54
Superior corona radiata R	0.29	<**0.01**	0.31	0.64	0.13	0.54
Superior corona radiata L	0.52	0.14	0.23	0.64	0.49	0.54
Posterior corona radiata R	0.46	0.05	0.17	0.64	0.39	0.54
Posterior corona radiata L	0.52	0.21	0.16	0.64	0.54	0.54

	p-value			*q*-value		
Regions of interest	**Asymptote**	**Delay**	**exp(−Speed)**	**Asymptote**	**Delay**	**exp(−Speed)**
Posterior thalamic radiation include optic radiation R	0.10	0.27	0.08	0.64	0.54	0.54
Posterior thalamic radiation include optic radiation L	0.26	0.83	0.09	0.64	0.94	0.54
External capsule R	0.02	0.18	**<0.01**	0.429	0.54	0.10
External capsule L	0.13	0.90	0.35	0.64	0.94	0.57
Superior longitudinal fasciculus R	0.34	0.94	0.19	0.64	0.94	0.54
Superior longitudinal fasciculus L	0.54	0.51	0.56	0.64	0.83	0.75

There were no group differences for FA between singletons and twins in terms of Gompertz parameters after multiple comparisons correction.

q-values are based on the false discovery rate adjustment of *p*-values.

TABLE AII

P-values for singleton–twin comparison of radial diffusivity (RD)

	p-value			*q*-value		
Regions of interest	**Asymptote**	**Delay**	**exp(−Speed)**	**Asymptote**	**Delay**	**exp(−Speed)**
Genu of corpus callosum	0.24	0.35	0.09	0.67	0.71	0.17
Body of corpus callosum	0.70	0.65	0.20	0.74	0.80	0.32
Splenium of corpus callosum	0.54	0.62	0.22	0.67	0.80	0.32
Anterior limb of internal capsule R	0.26	0.72	0.24	0.67	0.80	0.32
Anterior limb of internal capsule L	0.54	0.22	0.45	0.67	0.71	0.56
Posterior limb of internal capsule R	0.69	0.34	0.87	0.74	0.71	0.91
Posterior limb of internal capsule L	0.46	0.92	0.73	0.67	0.97	0.80
Retrolenticular part of internal capsule R	0.27	0.86	0.16	0.67	0.96	0.27
Retrolenticular part of internal capsule L	0.53	0.47	0.92	0.67	0.71	0.92
Anterior corona radiata R	0.41	0.22	**0.04**	0.67	0.71	0.17
Anterior corona radiata L	0.65	0.06	0.07	0.74	0.71	0.17
Superior corona radiata R	0.28	0.17	**0.03**	0.67	0.71	0.17
Superior corona radiata L	0.36	0.21	**0.03**	0.67	0.71	0.17
Posterior corona radiata R	0.52	0.25	0.09	0.67	0.71	0.17
Posterior corona radiata L	0.33	0.37	**0.03**	0.67	0.71	0.17
Posterior thalamic radiation include optic radiation R	0.26	0.47	0.09	0.67	0.71	0.17
Posterior thalamic radiation include optic radiation L	0.15	0.97	**0.04**	0.67	0.97	0.17
External capsule R	0.17	0.18	0.09	0.67	0.71	0.17
External capsule L	0.33	0.40	0.23	0.67	0.71	0.32
Superior longitudinal fasciculus R	0.44	0.54	0.08	0.67	0.76	0.17
Superior longitudinal fasciculus L	0.79	0.46	0.37	0.79	0.71	0.45

There were no group differences for RD between singletons and twins in terms of Gompertz parameters after multiple comparisons correction.

q-values are based on the false discovery rate adjustment of *p*-values.

TABLE AIII

P-values for singleton–twin comparison of axial diffusivity (AD)

	p-value			*q*-value		
Regions of interest	**Asymptote**	**Delay**	**exp(−Speed)**	**Asymptote**	**Delay**	**exp(−Speed)**
Genu of corpus callosum	0.25	0.10	0.92	0.96	0.16	0.92
Body of corpus callosum	0.13	0.87	0.01	0.96	0.91	0.29
Splenium of corpus callosum	0.21	0.67	0.05	0.96	0.74	0.41
Anterior limb of internal capsule R	0.37	**<0.01**	0.72	0.96	**<0.01**	0.75
Anterior limb of internal capsule L	0.88	**<0.01**	0.28	0.96	**<0.01**	0.41
Posterior limb of internal capsule R	0.22	0.64	0.09	0.96	0.74	0.41
Posterior limb of internal capsule L	0.71	0.91	0.41	0.96	0.91	0.54
Retrolenticular part of internal capsule R	0.77	0.08	0.18	0.96	0.13	0.41
Retrolenticular part of internal capsule L	0.91	0.21	0.65	0.96	0.26	0.72
Anterior corona radiata R	0.60	**<0.01**	0.16	0.96	**0.02**	0.41
Anterior corona radiata L	0.36	**<0.01**	0.29	0.96	**0.02**	0.41
Superior corona radiata R	0.64	0.05	0.15	0.96	0.09	0.41
Superior corona radiata L	0.74	**0.02**	0.24	0.96	0.07	0.41
Posterior corona radiata R	0.96	0.15	0.19	0.96	0.19	0.41
Posterior corona radiata L	0.49	0.15	0.07	0.96	0.19	0.41
Posterior thalamic radiation include optic radiation R	0.63	**0.02**	0.44	0.96	0.07	0.54
Posterior thalamic radiation include optic radiation L	0.72	0.07	0.27	0.96	0.12	0.41
External capsule R	0.92	**0.03**	0.27	0.96	0.07	0.41
External capsule L	0.55	**0.01**	0.63	0.96	0.06	0.72
Superior longitudinal fasciculus R	0.96	**0.03**	0.27	0.96	0.07	0.41
Superior longitudinal fasciculus L	0.90	**0.04**	0.16	0.96	0.09	0.41

There were significant group differences in the delay parameter of Gompertz function for AD between singletons and twins after multiple comparisons correction in the anterior limb of the internal capsule and the anterior corona radiata.

q-values are based on the false discovery rate adjustment of *p*-values.

TABLE AIV

Effect size of singleton–twin comparison of fractional anisotropy (FA)

	Asymptote	**Delay**	**exp(−Speed)**
Genu of corpus callosum	0.12	0.05	0.17
Body of corpus callosum	−0.09	0.07	0.02
Splenium of corpus callosum	−0.08	−0.13	<0.01
Anterior limb of internal capsule R	0.31	0.30	0.19
Anterior limb of internal capsule L	0.20	−0.01	0.10
Posterior limb of internal capsule R	−0.11	−0.19	−0.02
Posterior limb of internal capsule L	0.17	−0.18	<0.01
Retrolenticular part of internal capsule R	0.16	0.03	0.05

	Asymptote	Delay	exp(−Speed)
Retrolenticular part of internal capsule L	−0.08	0.09	−0.05
Anterior corona radiata R	0.10	−0.25	0.17
Anterior corona radiata L	0.08	−0.29	0.20
Superior corona radiata R	0.17	−0.45	0.17
Superior corona radiata L	0.10	−0.24	0.20
Posterior corona radiata R	0.12	−0.32	0.22
Posterior corona radiata L	0.10	−0.20	0.23
Posterior thalamic radiation include optic radiation R	0.27	−0.18	0.29
Posterior thalamic radiation include optic radiation L	0.18	−0.03	0.28
External capsule R	0.37	−0.23	0.50
External capsule L	0.25	−0.02	0.15
Superior longitudinal fasciculus R	0.16	−0.01	0.22
Superior longitudinal fasciculus L	0.10	−0.11	0.09

TABLE AV

Effect size of singleton–twin comparison of radial diffusivity (RD)

	Asymptote	Delay	exp(−Speed)
Genu of corpus callosum	−0.19	−0.15	0.28
Body of corpus callosum	−0.06	0.07	0.21
Splenium of corpus callosum	−0.10	0.08	0.20
Anterior limb of internal capsule R	−0.18	0.06	0.19
Anterior limb of internal capsule L	−0.10	0.20	0.11
Posterior limb of internal capsule R	0.06	0.16	0.03
Posterior limb of internal capsule L	−0.12	0.02	0.06
Retrolenticular part of internal capsule R	−0.19	−0.03	0.23
Retrolenticular part of internal capsule L	0.10	0.12	0.02
Anterior corona radiata R	−0.13	0.20	0.33
Anterior corona radiata L	−0.07	0.30	0.30
Superior corona radiata R	−0.18	0.22	0.35
Superior corona radiata L	−0.15	0.20	0.35
Posterior corona radiata R	−0.10	0.19	0.28
Posterior corona radiata L	−0.16	0.15	0.35
Posterior thalamic radiation include optic radiation R	−0.18	0.12	0.28
Posterior thalamic radiation include optic radiation L	−0.23	0.01	0.34
External capsule R	−0.22	0.22	0.28
External capsule L	−0.16	0.14	0.19
Superior longitudinal fasciculus R	−0.12	0.10	0.28
Superior longitudinal fasciculus L	−0.04	0.12	0.15

TABLE AVI

Effect size of singleton–twin comparison of axial diffusivity (AD)

	Asymptote	Delay	exp(−Speed)
Genu of corpus callosum	0.19	0.27	−0.02
Body of corpus callosum	−0.24	0.03	0.41
Splenium of corpus callosum	−0.20	0.07	0.33
Anterior limb of internal capsule R	0.15	**0.75**	0.06
Anterior limb of internal capsule L	0.03	**0.59**	0.18
Posterior limb of internal capsule R	−0.20	−0.07	0.29
Posterior limb of internal capsule L	0.06	0.02	0.14
Retrolenticular part of internal capsule R	0.05	0.28	0.22
Retrolenticular part of internal capsule L	−0.02	0.21	0.07
Anterior corona radiata R	0.09	**0.48**	0.23
Anterior corona radiata L	0.15	**0.49**	0.17
Superior corona radiata R	0.07	0.33	0.23
Superior corona radiata L	0.05	0.38	0.19
Posterior corona radiata R	0.01	0.24	0.22
Posterior corona radiata L	−0.11	0.24	0.30
Posterior thalamic radiation include optic radiation R	0.08	0.38	0.13
Posterior thalamic radiation include optic radiation L	−0.06	0.29	0.18
External capsule R	0.02	0.36	0.18
External capsule L	0.10	0.40	0.08
Superior longitudinal fasciculus R	0.01	0.36	0.18
Superior longitudinal fasciculus L	−0.02	0.33	0.23

The numbers in bold correspond to regions that were significantly different between twins and singletons.

APPENDIX B

SIMULATION RESULTS FOR MISSING DATA

We performed a Monte Carlo simulation based on synthetic longitudinal data. The data were generated based on the estimated model parameters for FA values of all ROIs (Table V). Age of subjects were also randomly selected based on the min/max of each age group to resemble the data in our study. The full sample contained 26 twin subjects and 26 singleton subjects, each with three time-points. The reduced dataset was the same data as above, except treating 13 twin subjects and 13 singleton subjects as dropouts by discarding their last time-point. We had 1000 random simulation, and the results are presented in Table AVII. The missing time-points have minor effect on the estimated fixed effect parameters of the Gompertz function.

TABLE AVII

The influence of missing time-points on the estimated fixed-effect parameters of the Gompertz function

	Values used for simulation Input parameters	Estimated parameters	
		Full dataset	Reduced dataset
Singletons			
Asymptote	0.412 (0.006)	0.410 (0.006)	0.411 (0.006)
Delay	0.591 (0.022)	0.599 (0.021)	0.599 (0.022)
Exp(−speed) × 10^2	99.583 (0.0004)	99.581 (0.0004)	99.582 (0.0004)
Twins			
Asymptote	0.405 (0.007)	0.403 (0.008)	0.403 (0.008)
Delay	0.617 (0.026)	0.625 (0.026)	0.626(0.026)
Exp(−speed) × 10^2	99.532 (0.0004)	99.532 (0.0004)	99.532 (0.0004)

REFERENCES

Akaike H. A new look at the statistical model identification. IEEE Trans Auto Control. 1974; 19:716–723.

Alexander D, Pierpaoli C, Basser P, Gee J. Spatial transformations of diffusion tensor magnetic resonance images. IEEE Trans Med Imaging. 2001; 20:1131–1139. [PubMed: 11700739]

Basser PJ, Mattiello J, LeBihan D. Estimation of the effective self-diffusion tensor from the NMR spin echo. J Magn Reson B. 1994; 103:247–254. [PubMed: 8019776]

Benjamini Y, Hochberg Y. Controlling the false discovery rate: A practical and powerful approach to multiple testing. J R Stat Soc B (Methodological). 1995; 57:289–300.

Bernal-Rusiel JL, Greve DN, Reuter M, Fischl B, Sabuncu MR. Statistical analysis of longitudinal neuroimage data with linear mixed effects models. NeuroImage. 2013; 66:249–260. URL http://www.sciencedirect.com/science/article/pii/S1053811912010683. [PubMed: 23123680]

Buckler J, Green M. A comparison of the early growth of twins and singletons. Ann Hum Biol. 2004; 31:311–332. [PubMed: 15204347]

Chen, Y.; Zhu, H.; Shen, D.; An, H.; Gilmore, J.; Lin, W. Medical Image Computing and Computer-Assisted Intervention-MICCAI 2009. Springer; 2009. Mapping growth patterns and genetic influences on early brain development in twins; p. 232-239.

Chiang MC, McMahon KL, de Zubicaray GI, Martin NG, Hickie I, Toga AW, Wright MJ, Thompson PM. Genetics of white matter development: A DTI study of 705 twins and their siblings aged 12 to 29. Neuroimage. 2011; 54:2308–2317. [PubMed: 20950689]

Christensen K, Petersen I, Skytthe A, Herskind AM, McGue M, Bingley P. Comparison of academic performance of twins and singletons in adolescence: Follow-up study. BMJ. 2006; 333:1095. [PubMed: 17012267]

Diggle, P.; Heagerty, P.; Liang, K.; Zeger, S. Analysis of Longitudinal Data. 2nd. New York: Oxford University Press; 2002.

Dubois J, Dehaene-Lambertz G, Perrin M, Mangin J, Cointepas Y, Duchesnay E, Le Bihan D, Hertz-Pannier L. Asynchrony of the early maturation of white matter bundles in healthy infants: Quantitative landmarks revealed noninvasively by diffusion tensor imaging. Hum Brain Mapp. 2008; 29:14–27. [PubMed: 17318834]

Fletcher P, Joshi S. Riemannian geometry for the statistical analysis of diffusion tensor data. Signal Process. 2007; 87:250–262.

Gao W, Lin W, Chen Y, Gerig G, Smith JK, Jewells V, Gilmore J. Temporal and spatial development of axonal maturation and myelination of white matter in the developing brain. AJNR Am J Neuroradiol. 2009; 30:290–296. [PubMed: 19001533]

Geng X, Gouttard S, Sharma A, Gu H, Styner M, Lin W, Gerig G, Gilmore JH. Quantitative tract-based white matter development from birth to age 2years. NeuroImage. 2012; 61:542–557. [PubMed: 22510254]

Gilmore JH, Schmitt JE, Knickmeyer RC, Smith JK, Lin W, Styner M, Gerig G, Neale MC. Genetic and environmental contributions to neonatal brain structure: A twin study. Hum Brain Mapp. 2010; 31:1174–1182. [PubMed: 20063301]

Hay DA, O'Brien PJ. The La Trobe Twin Study: A genetic approach to the structure and development of cognition in twin children. Child Dev. 1983; 54:317–330. [PubMed: 6683618]

Hermoye L, Saint-Martin C, Cosnard G, Lee SK, Kim J, Nassogne MC, Menten R, Clapuyt P, Donohue PK, Hua K, Wakana S, Jiang H, van Zijl PC, Mori S. Pediatric diffusion tensor imaging: Normal database and observation of the white matter maturation in early childhood. NeuroImage. 2006; 29:493–504. [PubMed: 16194615]

Hulshoff Pol HE, Posthuma D, Baare WF, De Geus EJ, Schnack HG, van Haren NE, van Oel CJ, Kahn RS, Boomsma DI. Twin–singleton differences in brain structure using structural equation modelling. Brain. 2002; 125(Pt 2):384–390. [PubMed: 11844738]

Huppi P, Maier S, Peled S, Zientara G, Barnes P, Jolesz F, Volpe JJ. Microstructural development of human newborn cerebral white matter assessed in vivo by diffusion tensor magnetic resonance imaging. Pediatr Res. 1998; 44:584–590. [PubMed: 9773850]

Jahanshad N, Kochunov PV, Sprooten E, Mandl RC, Nichols TE, Almasy L, Blangero J, Brouwer RM, Curran JE, de Zubicaray GI, et al. Multi-site genetic analysis of diffusion images and voxelwise heritability analysis: A pilot project of the enigma–DTI working group. Neuroimage. 2013; 81:455–469. [PubMed: 23629049]

Jones DK. The effect of gradient sampling schemes on measures derived from diffusion tensor MRI: A Monte Carlo study. Magn Reson Med. 2004; 51:807–815. [PubMed: 15065255]

Joshi S, Davis B, Jomier M, Gerig G. Unbiased diffeomorphic atlas construction for computational anatomy. Neuro-Image. 2004; 23:S151–S160. [PubMed: 15501084]

Kendler KS. Twin studies of psychiatric illness: An update. Arch Gen Psychiatry. 2001; 58:1005–1014. [PubMed: 11695946]

Knickmeyer RC, Kang C, Woolson S, Smith JK, Hamer RM, Lin W, Gerig G, Styner M, Gilmore JH. Twin-singleton differences in neonatal brain structure. Twin Res Hum Genet. 2011; 14:268–276. [PubMed: 21623657]

Lee SJ, Steiner RJ, Luo S, Neale MC, Styner M, Zhu H, Gilmore JH. Quantitative tract-based white matter heritability in twin neonates. NeuroImage. 2015; 111:123–135. [PubMed: 25700954]

Lindstrom M, Bates D. Nonlinear mixed effects models for repeated measures data. Biometrics. 1990; 46:673–687. [PubMed: 2242409]

Mori S, Oishi K, Jiang H, Jiang L, Li X, Akhter K, Hua K, Faria A, Mahmood A, Woods R, Toga A, Pike G, Neto P, Evans A, Zhang J, Huang H, Miller M, van Zijl P, Mazziotta J. Stereotaxic white matter atlas based on diffusion tensor imaging in an ICBM template. NeuroImage. 2008; 40:570–582. [PubMed: 18255316]

Mukherjee P, Miller J, Shimony J, Philip J, Nehra D, Snyder A, Conturo T, Neil J, McKinstry R. Diffusion-tensor MR imaging of gray and white matter development during normal human brain maturation. AJNR Am J Neuroradiol. 2002; 23:1445–1456. [PubMed: 12372731]

Nathan M, Guttman R. Similarities in test scores and profiles of kibbutz twins and singletons. Acta Genet Med Gemellol (Roma). 1984; 33:213–218. [PubMed: 6540953]

Ni H, Kavcic V, Zhu T, Ekholm S, Zhong J. Effects of number of diffusion gradient directions on derived diffusion tensor imaging indices in human brain. AJNR Am J Neuroradiol. 2006; 27:1776–1781. [PubMed: 16971635]

Ordaz SJ, Lenroot RK, Wallace GL, Clasen LS, Blumenthal JD, Schmitt JE, Giedd JN. Are there differences in brain morphometry between twins and unrelated singletons? A pediatric MRI study. Genes Brain Behav. 2010; 9:288–295. [PubMed: 20100212]

Pennec X, Fillard P, Ayache N. A riemannian framework for tensor computing. Int J Comput Vis. 2006; 66:41–66.

Peper JS, Brouwer RM, Boomsma DI, Kahn RS, Pol H, Hilleke E. Genetic influences on human brain structure: A review of brain imaging studies in twins. Hum Brain Mapp. 2007; 28:464–473. [PubMed: 17415783]

Pierpaoli C, Jezzard P, Basser PJ, Barnett A, Di Chiro G. Diffusion tensor MR imaging of the human brain. Radiology. 1996; 201:637–648. [PubMed: 8939209]

Pinheiro, JC. PhD thesis. University of Wisconsin, Madison; 1994. Topics in mixed effects models.

Posthuma D, De Geus EJ, Bleichrodt N, Boomsma DI. Twin-singleton differences in intelligence? Twin Res. 2000; 3:83–87. [PubMed: 10918620]

Rueckert D, Sonoda L, Hayes C, Hill D, Leach M, Hawkes D. Nonrigid registration using free-form deformations: Application to breast MR images. IEEE Trans Med Imaging. 1999; 18:712–721. [PubMed: 10534053]

Sadeghi, N. PhD thesis. University of Utah; 2013. Modeling and analysis of longitudinal multimodal magnetic resonance imaging: Application to early brain development.

Sadeghi N, Prastawa M, Fletcher PT, Wolff J, Gilmore JH, Gerig G. Regional characterization of longitudinal DT-MRI to study white matter maturation of the early developing brain. Neuroimage. 2013; 68:236–247. [PubMed: 23235270]

Salvador R, Pena A, Menon D, Carpenter T, Pickard J, Bullmore E. Formal characterization and extension of the linearized diffusion tensor model. Hum Brain Mapp. 2005; 24:144–155. [PubMed: 15468122]

Smith SM. Fast robust automated brain extraction. Hum Brain Mapp. 2002; 17:143–155. [PubMed: 12391568]

Wilson RS. Growth standards for twins from birth to four years. Ann Hum Biol. 1974; 1:175–188. [PubMed: 4472129]

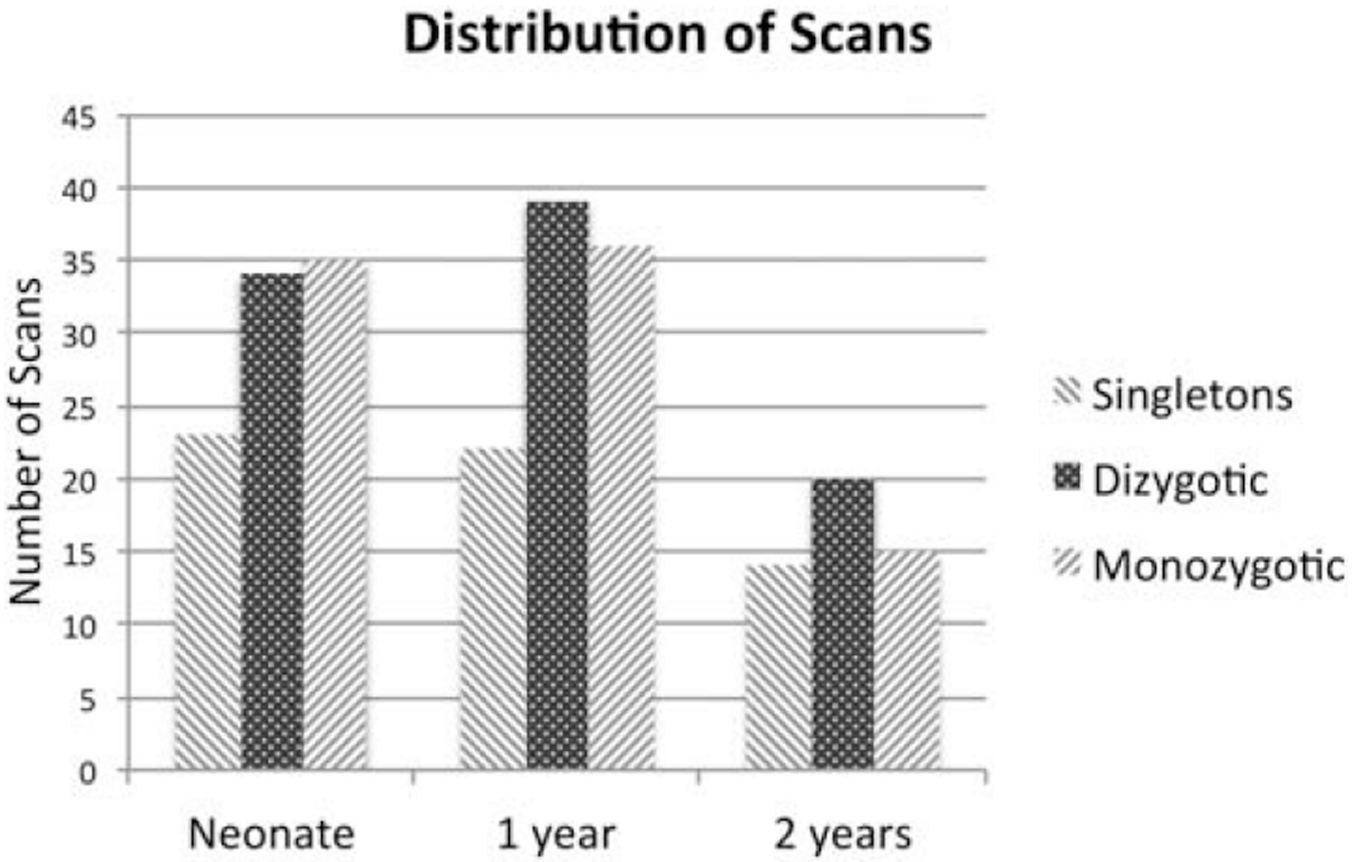

	Neonate	1 year	2 years	Total
Singletons	23	22	14	59
Dizygotic	34	39	20	93
Monozygotic	35	36	15	86
Total	92	97	49	238

Figure 1.
Distribution of scans. [Color figure can be viewed at wileyonlinelibrary.com]

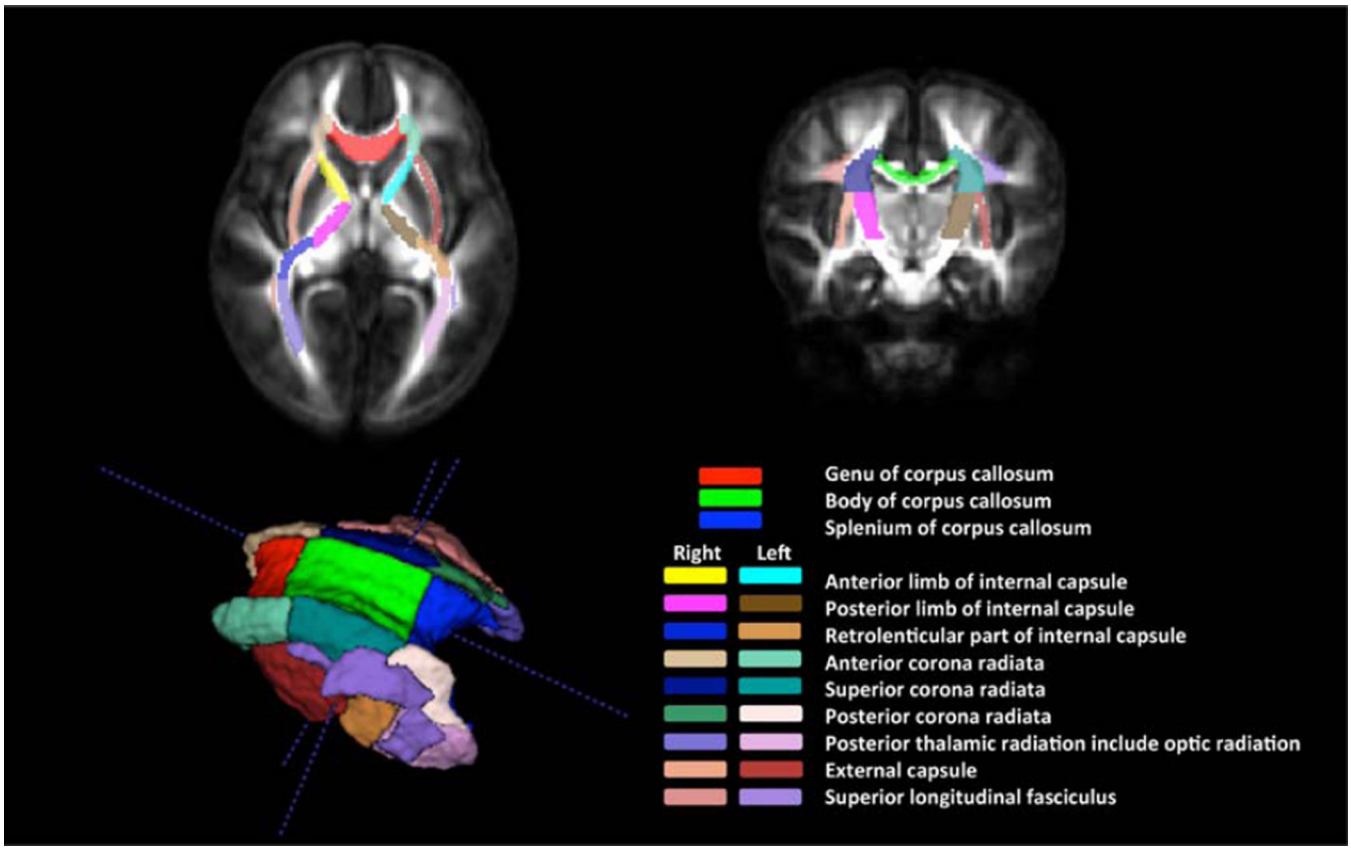

Figure 2.

White matter anatomical labels that are used for regional analysis. Top: Labels are overlaid on the FA map of the reference space that is the population atlas. Bottom: 3d representation of regions of interest.

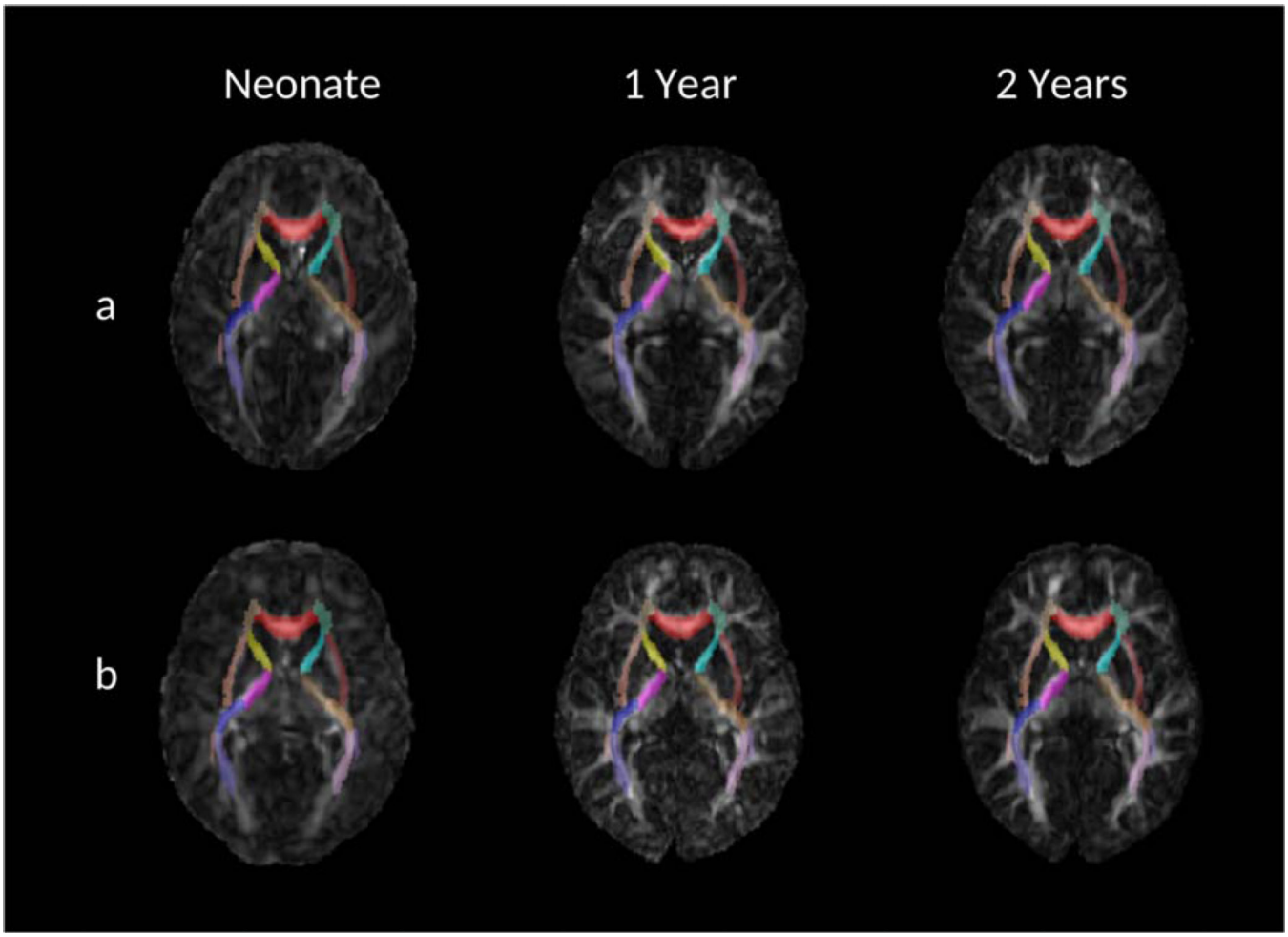

Figure 3.
White matter anatomical labels are overlaid on the FA scans of (a) singleton subject and (b) twin subject.

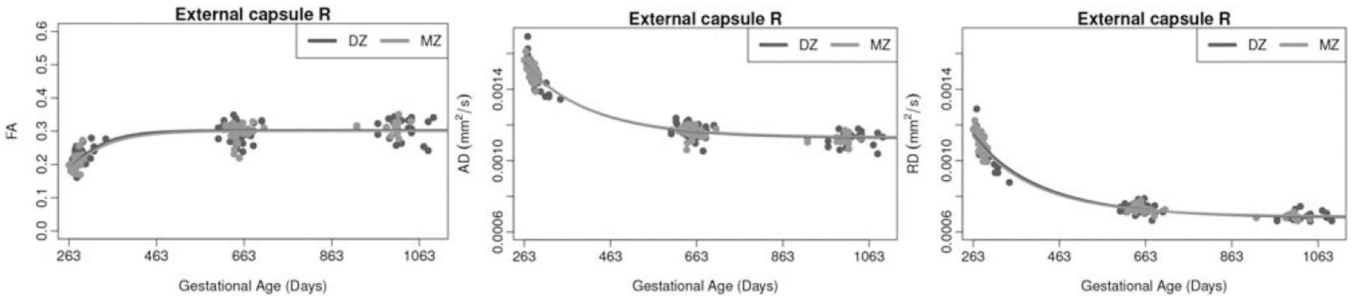

Figure 4.

Comparison of FA, AD, and RD growth trajectories of monozygotic (MZ) and dizygotic (DZ) twins for the right external capsule, where the average growth trajectories almost overlap. [Color figure can be viewed at wileyonlinelibrary.com]

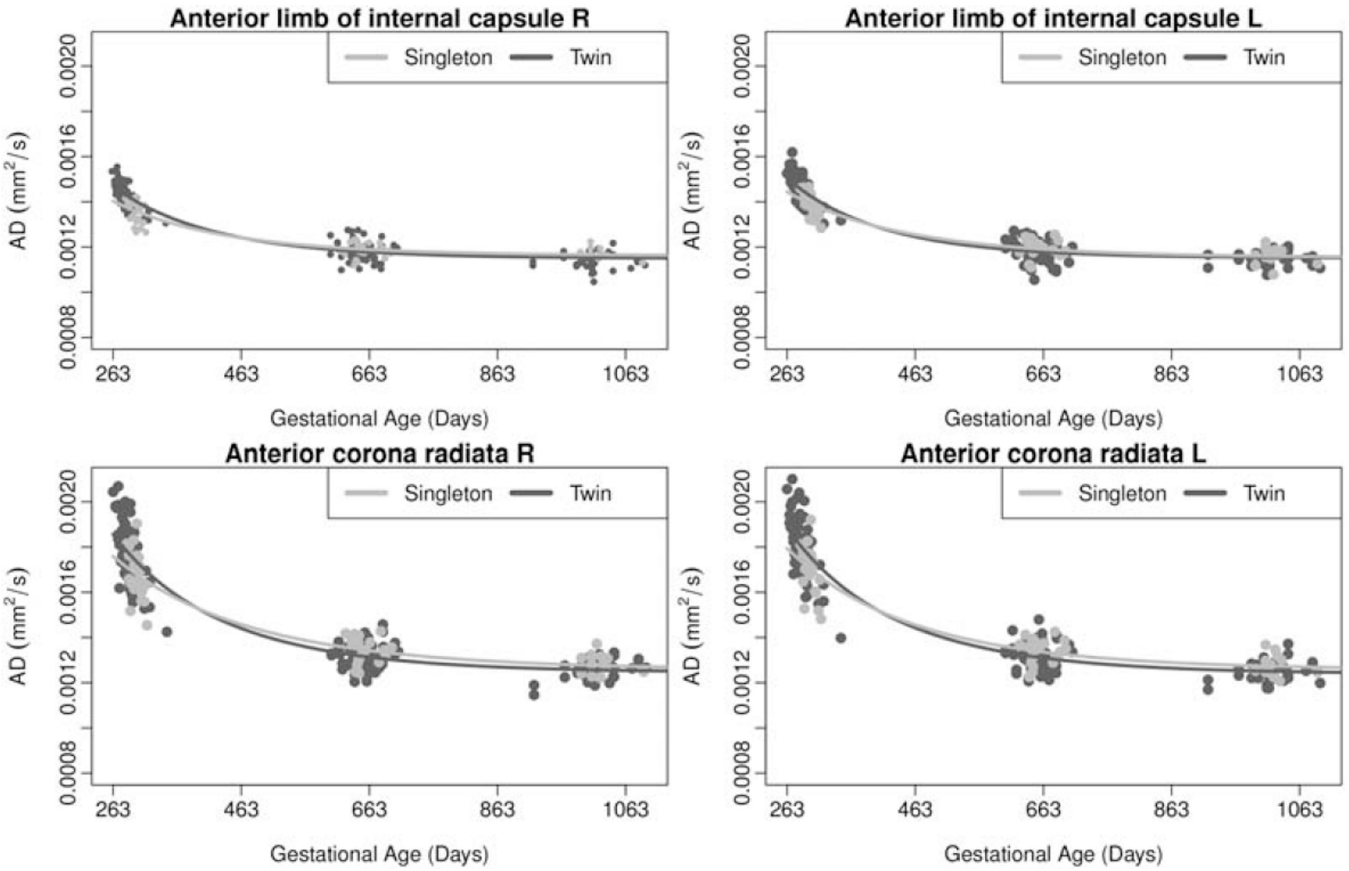

Figure 5.

Comparison of AD growth trajectories of twins and singletons for the anterior limb of the internal capsule and the anterior corona radiata. The delay parameter was significantly different between twins and singletons in these regions (higher values for AD at an earlier gestational age). [Color figure can be viewed at wileyonlinelibrary.com]

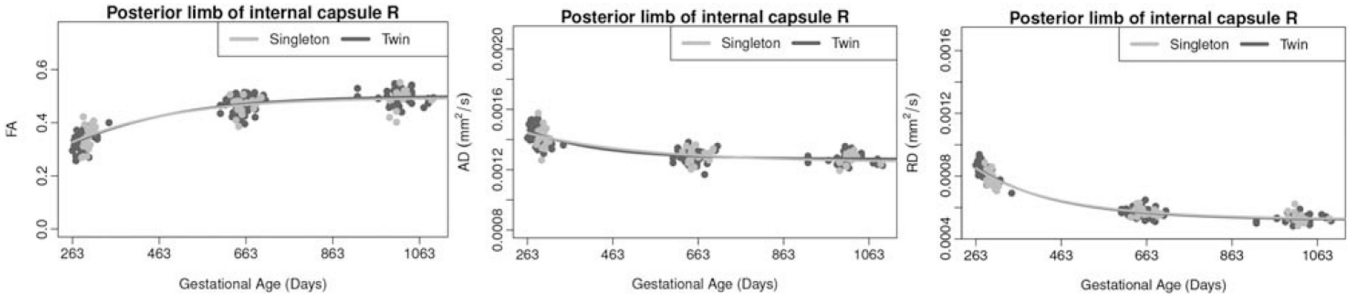

Figure 6.

Comparison of FA, AD, and RD growth trajectory of twins and singletons. There were no significant differences between twin and singleton trajectories in the posterior limb of the internal capsule. [Color figure can be viewed at wileyonlinelibrary.com]

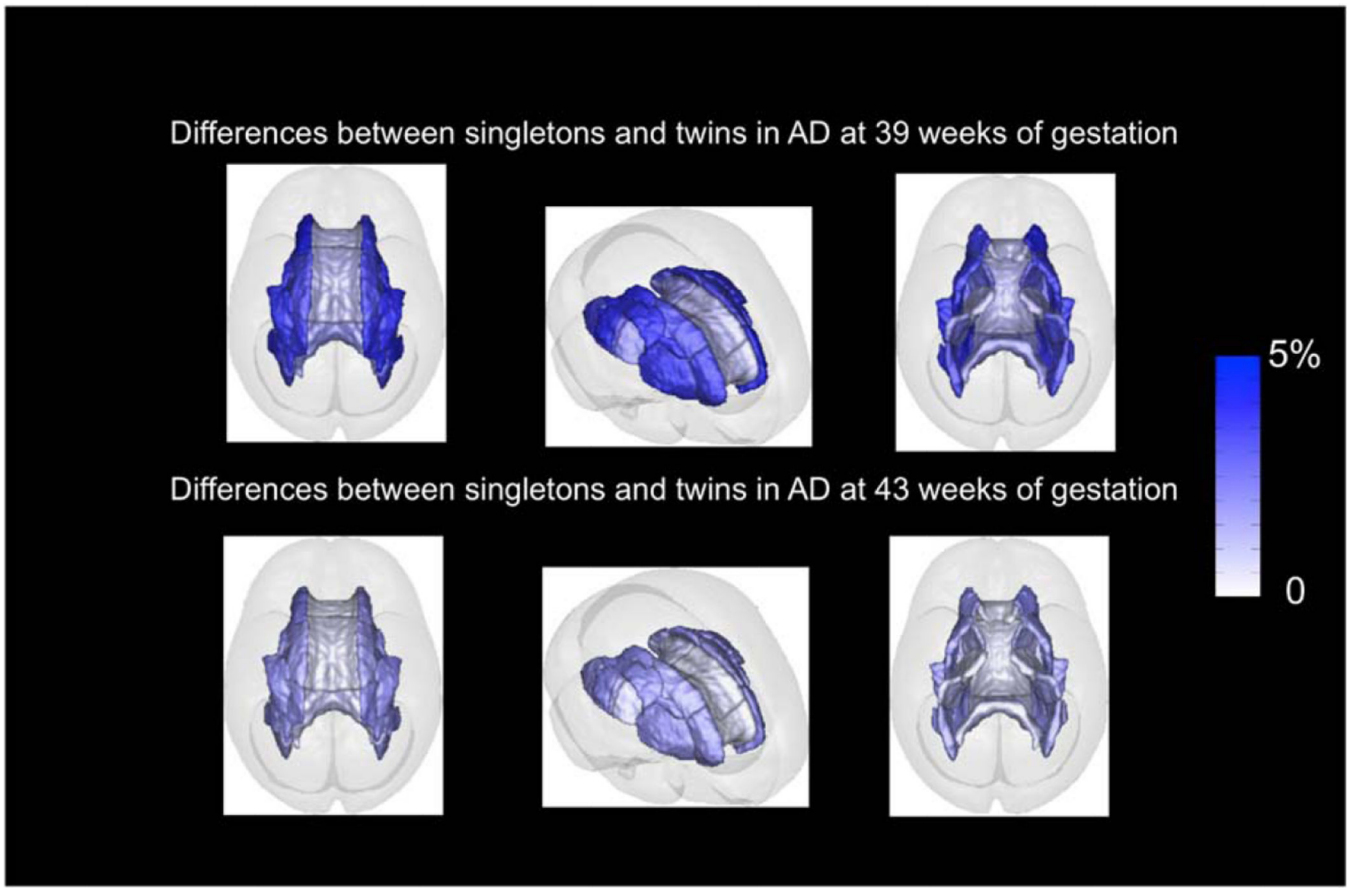

Figure 7.

Differences in axial diffusivity (AD) of twins versus singletons ((Twin – Singleton)/Singleton). Top: Differences in AD between twins and singletons at 39 weeks of gestation. Bottom: Differences at 43 weeks of gestation. The changes from dark blue at birth to light blue at 43 weeks of gestation indicate that differences between twins and singletons quickly become much smaller and reach the same white matter maturation values.

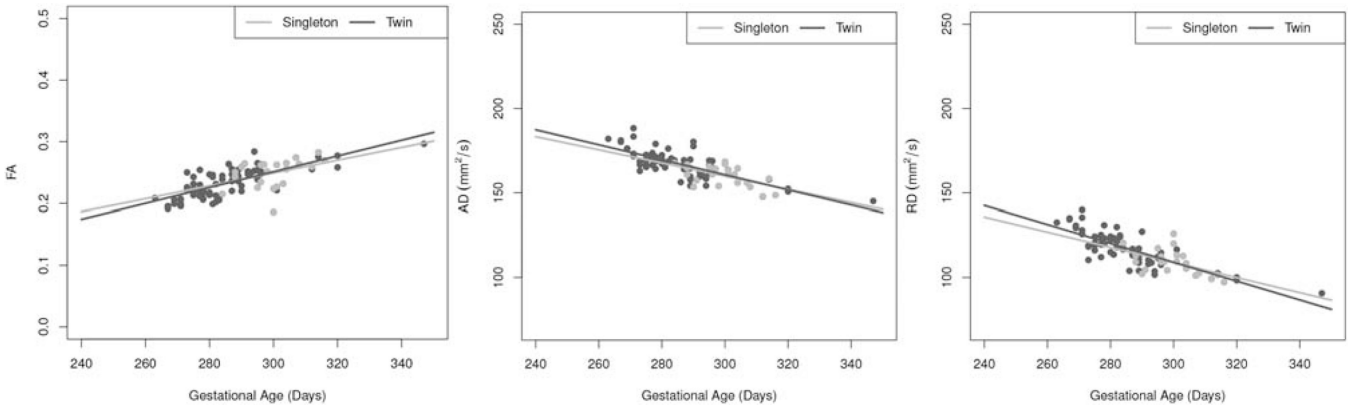

Figure 8.

Comparison of FA, AD, and RD of twins and singletons at the earliest time point. There were no significant differences between twins and singletons for any of the measurements. [Color figure can be viewed at wileyonlinelibrary.com]

TABLE I

Demographic data

	Singletons	DZ	MZ
Female	11	19	18
Male	15	21	18
Gestation age at birth (standard deviation)	276.73 (8.86)	249.78 (14.36)	244.39 (22.12)
Gestation age at first MRI[a] (standard deviation)	298.04 (9.96)	289.73 (16.82)	280.56 (8.71)

[a]Not all subjects had their first MRI at neonate. The mean and standard deviation of gestational age is calculated for the subjects with available MRI at neonate.

TABLE II

Singleton–twin comparison of fractional anisotropy (FA)

	Singleton			Twin		
Regions of interest	**Asymptote (SE)**	**Delay (SE)**	**exp(−Speed) (SE) ×10^{-2}**	**Asymptote (SE)**	**Delay (SE)**	**exp(−Speed) (SE) ×10^{-2}**
Genu of corpus callosum	0.55 (0.02)	0.75 (0.04)	99.70 (0.04)	0.54 (0.02)	0.74 (0.04)	99.65 (0.04)
Body of corpus callosum	0.44 (0.01)	0.74 (0.03)	99.57 (0.05)	0.45 (0.02)	0.72 (0.03)	99.56 (0.06)
Splenium of corpus callosum	0.48 (0.01)	0.66 (0.02)	99.47 (0.07)	0.49 (0.01)	0.68 (0.03)	99.47 (0.07)
Anterior limb of internal capsule R	0.39 (0.01)	0.70 (0.03)	99.55 (0.06)	0.37 (0.01)	0.63 (0.04)	99.46 (0.08)
Anterior limb of internal capsule L	0.38 (0.01)	0.59 (0.04)	99.53 (0.09)	0.37 (0.01)	0.59 (0.04)	99.47 (0.10)
Posterior limb of internal capsule R	0.49 (0.01)	0.41 (0.02)	99.51 (0.09)	0.50 (0.01)	0.44 (0.03)	99.52 (0.10)
Posterior limb of internal capsule L	0.50 (0.01)	0.41 (0.02)	99.43 (0.10)	0.49 (0.01)	0.43 (0.02)	99.43 (0.12)
RLIC R	0.47 (0.01)	0.38 (0.03)	99.53 (0.11)	0.45 (0.01)	0.38 (0.03)	99.50 (0.13)
RLIC L	0.41 (0.01)	0.37 (0.03)	99.45 (0.16)	0.41 (0.02)	0.35 (0.03)	99.50 (0.18)
Anterior corona radiata R	0.37 (0.01)	0.88 (0.05)	99.58 (0.04)	0.36 (0.01)	0.97 (0.06)	99.53 (0.05)
Anterior corona radiata L	0.36 (0.01)	0.85 (0.04)	99.59 (0.04)	0.36 (0.01)	0.95 (0.05)	99.53 (0.04)
Superior corona radiata R	0.39 (0.01)	0.51 (0.03)	99.57 (0.08)	0.37 (0.01)	0.62 (0.04)	99.47 (0.09)
Superior corona radiata L	0.38 (0.01)	0.56 (0.03)	99.54 (0.08)	0.38 (0.01)	0.62 (0.04)	99.42 (0.10)
Posterior corona radiata R	0.35 (0.01)	0.65 (0.04)	99.54 (0.06)	0.34 (0.01)	0.74 (0.05)	99.44 (0.07)
Posterior corona radiata L	0.35 (0.01)	0.62 (0.04)	99.59 (0.07)	0.34 (0.01)	0.67 (0.04)	99.47 (0.08)
Posterior thalamic radiation R	0.46 (0.02)	0.62 (0.05)	99.66 (0.05)	0.43 (0.02)	0.68 (0.05)	99.54 (0.06)
Posterior thalamic radiation L	0.46 (0.02)	0.57 (0.04)	99.66 (0.06)	0.44 (0.02)	0.58 (0.04)	99.53 (0.07)
External capsule R	0.33 (0.01)	0.42 (0.03)	99.49 (0.13)	0.30 (0.01)	0.49 (0.05)	98.48 (0.35)
External capsule L	0.33 (0.01)	0.49 (0.03)	99.42 (0.14)	0.32 (0.01)	0.49 (0.03)	99.23 (0.20)
Superior longitudinal fasciculus R	0.38 (0.01)	0.79 (0.04)	99.59 (0.04)	0.37 (0.01)	0.79 (0.04)	99.52 (0.05)
Superior longitudinal fasciculus L	0.37 (0.01)	0.76 (0.04)	99.56 (0.05)	0.37 (0.01)	0.79 (0.05)	99.52 (0.06)

There were no group differences for FA between singletons and twins in terms of Gompertz parameters. RLIC: retrolenticular part of the internal capsule.

TABLE III

Singleton–twin comparison of radial diffusivity (RD)

	Singleton			Twin		
Regions of interest	**Asymptote (SE) ×10^{-5}**	**Delay (SE)**	**exp(−Speed) (SE) ×10^{-2}**	**Asymptote (SE) ×10^{-5}**	**Delay (SE)**	**exp(−Speed) (SE) ×10^{-2}**
Genu of corpus callosum	44.88 (6.17)	−1.00 (0.13)	99.87 (0.03)	52.75 (6.75)	−0.87 (0.14)	99.82 (0.03)
Body of corpus callosum	62.47 (2.43)	−0.67 (0.04)	99.72 (0.04)	63.53 (2.77)	−0.69 (0.04)	99.67 (0.04)
Splenium of corpus callosum	59.71 (1.77)	−0.72 (0.03)	99.65 (0.04)	60.97 (2.06)	−0.73 (0.03)	99.60 (0.04)
Anterior limb of internal capsule R	59.25 (0.96)	−0.56 (0.02)	99.60 (0.04)	60.52 (1.13)	−0.57 (0.02)	99.55 (0.04)
Anterior limb of internal capsule L	60.20 (1.09)	−0.55 (0.02)	99.59 (0.04)	60.99 (1.27)	−0.58 (0.02)	99.55 (0.05)
Posterior limb of internal capsule R	52.26 (0.90)	−0.49 (0.02)	99.57 (0.05)	51.84 (1.08)	−0.51 (0.02)	99.56 (0.05)
Posterior limb of internal capsule L	52.32 (0.77)	−0.50 (0.01)	99.53 (0.05)	53.00 (0.92)	−0.50 (0.02)	99.51 (0.06)
RLIC R	59.92 (1.60)	−0.51 (0.03)	99.65 (0.05)	62.05 (1.83)	−0.51 (0.03)	99.56 (0.06)
RLIC L	65.13 (1.27)	−0.46 (0.02)	99.55 (0.06)	64.16 (1.53)	−0.48 (0.02)	99.54 (0.07)
Anterior corona radiata R	66.96 (1.77)	−0.74 (0.03)	99.67 (0.03)	68.64 (2.01)	−0.79 (0.04)	99.60 (0.04)
Anterior corona radiata L	68.20 (1.50)	−0.73 (0.03)	99.65 (0.03)	69.00 (1.73)	−0.79 (0.03)	99.58 (0.03)
Superior corona radiata R	61.36 (1.85)	−0.62 (0.03)	99.66 (0.04)	63.61 (2.07)	−0.67 (0.04)	99.55 (0.05)
Superior corona radiata L	62.00 (1.78)	−0.63 (0.03)	99.66 (0.04)	63.83 (1.98)	−0.68 (0.04)	99.54 (0.05)
Posterior corona radiata R	73.38 (2.02)	−0.64 (0.03)	99.62 (0.05)	74.87 (2.30)	−0.69 (0.04)	99.52 (0.06)
Posterior corona radiata L	72.27 (2.07)	−0.63 (0.03)	99.64 (0.05)	74.53 (2.32)	−0.66 (0.04)	99.52 (0.06)
Posterior thalamic radiation R	65.07 (2.80)	−0.67 (0.04)	99.68 (0.05)	68.55 (3.07)	−0.70 (0.05)	99.56 (0.07)
Posterior thalamic radiation L	65.63 (2.46)	−0.66 (0.04)	99.67 (0.05)	69.52 (2.69)	−0.66 (0.04)	99.55 (0.06)
External capsule R	66.60 (0.83)	−0.50 (0.01)	99.56 (0.04)	67.92 (0.96)	−0.52 (0.02)	99.49 (0.05)
External capsule L	66.81 (1.03)	−0.52 (0.01)	99.55 (0.05)	67.97 (1.19)	−0.53 (0.02)	99.48 (0.06)
Superior longitudinal fasciculus R	65.64 (1.61)	−0.69 (0.03)	99.64 (0.03)	67.07 (1.85)	−0.71 (0.03)	99.57 (0.04)
Superior longitudinal fasciculus L	66.78 (1.43)	−0.67 (0.03)	99.61 (0.04)	67.23 (1.69)	−0.69 (0.03)	99.57 (0.04)

There were no group differences for RD between singletons and twins in terms of Gompertz parameters. RLIC: retrolenticular part of the internal capsule.

TABLE IV

Singleton–twin comparison of axial diffusivity (AD)

Regions of interest	Singleton			Twin		
	Asymptote (SE) $\times 10^{-5}$	Delay (SE)	exp(−Speed) (SE) $\times 10^{-2}$	Asymptote (SE) $\times 10^{-5}$	Delay (SE)	exp(−Speed) (SE) $\times 10^{-2}$
Genu of corpus callosum	155.46 (4.12)	−0.19 (0.03)	99.80 (0.05)	149.71 (4.99)	−0.24 (0.03)	99.81 (0.06)
Body of corpus callosum	136.13 (4.14)	−0.21 (0.03)	99.80 (0.06)	142.69 (4.37)	−0.21 (0.03)	99.62 (0.07)
Splenium of corpus callosum	145.00 (2.61)	−0.22 (0.02)	99.68 (0.06)	148.63 (2.90)	−0.23 (0.02)	99.51 (0.08)
Anterior limb of internal capsule R *	116.18 (1.19)	−0.19 (0.01)	99.47 (0.12)	114.91 (1.41)	−0.24 (0.01)	99.42 (0.14)
Anterior limb of internal capsule L *	115.34 (1.30)	−0.22 (0.01)	99.51 (0.09)	115.10 (1.51)	−0.27 (0.01)	99.39 (0.11)
Posterior limb of internal capsule R	124.75 (1.85)	−0.15 (0.01)	99.66 (0.09)	127.20 (2.00)	−0.14 (0.01)	99.41 (0.14)
Posterior limb of internal capsule L	126.61 (1.38)	−0.15 (0.01)	99.59 (0.10)	126.02 (1.58)	−0.15 (0.01)	99.49 (0.12)
RLIC R	135.48 (1.91)	−0.21 (0.01)	99.60 (0.08)	134.84 (2.18)	−0.23 (0.02)	99.47 (0.10)
RLIC L	131.10 (1.78)	−0.21 (0.01)	99.44 (0.12)	131.34 (2.14)	−0.23 (0.01)	99.38 (0.15)
Anterior corona radiata R *	125.71 (1.93)	−0.34 (0.02)	99.59 (0.06)	124.53 (2.23)	−0.40 (0.02)	99.50 (0.07)
Anterior corona radiata L *	125.74 (1.68)	−0.36 (0.02)	99.56 (0.05)	123.91 (1.99)	−0.42 (0.02)	99.49 (0.06)
Superior corona radiata R	118.63 (1.78)	−0.32 (0.02)	99.61 (0.05)	117.69 (2.03)	−0.36 (0.02)	99.52 (0.07)
Superior corona radiata L	118.67 (1.47)	−0.32 (0.02)	99.61 (0.04)	118.09 (1.73)	−0.37 (0.02)	99.55 (0.05)
Posterior corona radiata R	129.34 (2.02)	−0.35 (0.02)	99.57 (0.06)	129.22 (2.33)	−0.39 (0.02)	99.47 (0.08)
Posterior corona radiata L	126.13 (1.97)	−0.35 (0.02)	99.59 (0.05)	127.69 (2.26)	−0.39 (0.02)	99.47 (0.07)
Posterior thalamic radiation R	139.69 (2.70)	−0.27 (0.02)	99.55 (0.12)	138.20 (3.05)	−0.33 (0.03)	99.44 (0.14)
Posterior thalamic radiation L	140.37 (2.91)	−0.29 (0.02)	99.58 (0.11)	141.55 (3.23)	−0.33 (0.02)	99.44 (0.13)
External capsule R	112.68 (1.17)	−0.29 (0.01)	99.51 (0.06)	112.54 (1.37)	−0.32 (0.01)	99.43 (0.08)
External capsule L	114.69 (1.19)	−0.28 (0.01)	99.50 (0.07)	113.84 (1.41)	−0.31 (0.01)	99.46 (0.08)
Superior longitudinal fasciculus R	119.92 (1.59)	−0.33 (0.01)	99.55 (0.06)	119.81 (1.86)	−0.37 (0.02)	99.46 (0.07)
Superior longitudinal fasciculus L	119.49 (1.70)	−0.32 (0.01)	99.56 (0.07)	119.73 (1.94)	−0.36 (0.02)	99.44 (0.09)

* The delay parameter for AD for these regions was significantly different between singletons and twins based on the false discovery rate adjustment for multiple comparisons.

RLIC: retrolenticular part of the internal capsule.

TABLE V

Singleton–twin comparison of fractional anisotropy (FA), radial diffusivity (RD), and axial diffusivity (AD)

	Asymptote			Delay			exp(−Speed) ×10^{-2}		
Diffusion metric	**Singleton**	**Twins**	***p*-value**	**Singleton**	**Twins**	***p*-value**	**Singletons**	**Twins**	***p*-value**
FA	0.41	0.40	0.33	0.59	0.62	0.32	99.60	99.50	0.23
AD	128.30×10^{-5}	127.71×10^{-5}	0.61	−0.26	−0.30	< **0.01**	99.57	99.50	0.17
RD	64.84×10^{-5}	64.69×10^{-5}	0.51	−0.61	−0.64	0.19	99.63	99.58	0.10